

Rabi-coupling-induced three-component quantum droplet in ultracold Bose gases

Xiao Ding,^{1,2} Dajun Wang,³ and Xiaoling Cui¹

¹*Beijing National Laboratory for Condensed Matter Physics,
Institute of Physics, Chinese Academy of Sciences, Beijing 100190, China*

²*School of Physical Sciences, University of Chinese Academy of Sciences, Beijing 100049, China*

³*Department of Physics, The Chinese University of Hong Kong, Hong Kong, China*

(Dated: May 11, 2026)

We uncover a new mechanism for realizing three-component quantum droplets in ultracold Bose gases, where only one inter-species interaction is attractive. In this scheme, the inter-species attraction leads to a self-bound binary droplet, and the third component joins through Rabi coupling with one component of the binary droplet. We find that a stronger Rabi coupling leads to a larger fraction of the third component, but also destabilizes the entire droplet due to the involvement of more repulsive forces. Such instability can be remedied by a finite detuning between the Rabi-coupled components. We demonstrate these results in realistic Na-Rb mixtures, using both thermodynamic analyses and numerical simulations based on extended Gross-Pitaevskii equations. Our work outlines a general route for stabilizing multi-component droplets by bridging an existing binary droplet with additional components via suitable single-particle fields.

I. INTRODUCTION

Quantum droplets in ultracold atomic gases represent a novel state of matter characterized by their self-bound nature, where beyond-mean-field quantum fluctuations stabilize the system against collapse [1]. In recent years, quantum droplets have been successfully realized in both dipolar Bose gases [2–7] and alkali Bose-Bose mixtures [8–15]. In particular, a self-bound droplet of binary bosons has been shown to exhibit fascinating properties distinct from a repulsive Bose gas, including collective excitations [1, 16–20], low-dimensional behaviors [21–25], liquid-gas transition and coexistence [26–28], vortex structure [29–34], non-equilibrium dynamics [35–40], and interplay with spin-dependent fields [41–47] etc.

Beyond the framework of binary droplets, an interesting cutting-edge direction is droplet formation with multiple components. As a typical example, three-component droplets have been explored in both three dimensions (3D) [48–50] and one dimension (1D) [51, 52], where intriguing quantum phases, such as Borromean droplets [48] and shell-shaped droplets [49], have been revealed due to the interplay of mean-field interactions, quantum fluctuations, and spin degrees of freedom. Nevertheless, for three components to bind together as a droplet in 3D free space, at least two inter-species couplings must be attractive [48–50]. In practice, this requirement is very stringent, since in most realistic ultracold boson mixtures only one inter-species coupling can be tuned to be attractive at a given time. A natural question then arises: is it possible to bind three-component bosons into a droplet when attraction exists in only one inter-species channel? The present work aims to address this question.

Here, we propose a new mechanism for realizing three-component quantum droplets in ultracold boson mixtures with only one attractive inter-species coupling. Our scheme is illustrated in Fig. 1: for three-component (1,2,3) bosons, (1,2) form a binary droplet due to inter-

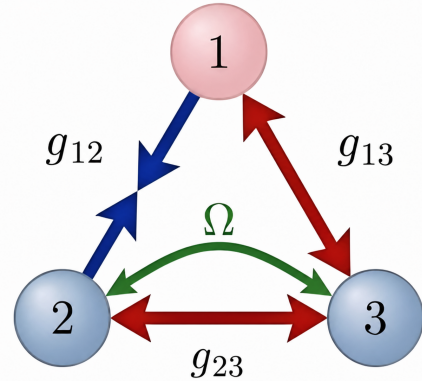


FIG. 1. Illustration for achieving a three-component (1,2,3) quantum droplet. Components 1 and 2 form a binary droplet in vacuum due to inter-species attraction, and component 3 joins via coherent Rabi coupling with component 2, thereby facilitating the formation of a (1,2,3) droplet. The coupling constants in all other interaction channels are repulsive.

species attraction, and the third component (3) joins via coherent Rabi coupling with one component (2) of the binary droplet. In this way, all three components can bind together as a self-bound droplet. Taking a realistic Na-Rb mixture as an example, we verify this proposal using both thermodynamic analyses and numerical simulations based on extended Gross-Pitaevskii equations. Interestingly, we find that a stronger Rabi coupling leads to a larger fraction of component 3, which, on the other hand, destabilizes the entire droplet due to the involvement of more repulsive forces. Such instability can be rescued by a finite detuning between the Rabi-coupled components (2 and 3). These results can be readily tested in current cold-atom experiments. Beyond the three-component droplet, our work also outlines a general route for stabilizing multi-component droplets—namely, by bridging an existing binary droplet with additional components via suitable single-particle fields.

The remainder of this paper is organized as follows. Section II presents our basic theoretical model. Section III is devoted to mean-field analysis. Section IV presents the main results on three-component quantum droplets, including their formation and stability in the thermodynamic limit, verification via extended GP equations, and the effect of magnetic detuning. The last section V provides the summary and outlook of this work.

II. MODEL

We write down the Hamiltonian of three-component (1,2,3) bosons in 3D as illustrated in Fig. 1: ($\hbar = 1$)

$$\begin{aligned} H &= \int d\mathbf{r} [H_0(\mathbf{r}) + U(\mathbf{r})], \\ H_0 &= -\sum_{i=1}^3 \psi_i^\dagger \frac{\nabla^2}{2m_i} \psi_i - \Omega(\psi_2^\dagger \psi_3 + h.c.) + \delta(\psi_2^\dagger \psi_2 - \psi_3^\dagger \psi_3); \\ U &= \frac{1}{2} \sum_{i,j=1}^3 g_{ij} \psi_i^\dagger \psi_j^\dagger \psi_j \psi_i. \end{aligned} \quad (1)$$

Here we have simplified the local field operators $\{\psi_i^\dagger(\mathbf{r}), \psi_i(\mathbf{r})\}$ as $\{\psi_i^\dagger, \psi_i\}$, which respectively create and annihilate a component- i boson with mass m_i at coordinate \mathbf{r} ; Ω and δ are respectively the strengths of Rabi coupling and detuning between components 2 and 3; $g_{ij} = 2\pi a_{ij}/m_{ij}$ is the interaction strength between components i and j , with scattering length a_{ij} and reduced mass $m_{ij} \equiv m_i m_j / (m_i + m_j)$. In this work, we consider all couplings to be repulsive except g_{12} , which is sufficiently negative to support a binary (1,2) droplet in vacuum [1].

As a specific example, we consider a realistic ultracold system of ^{23}Na - ^{87}Rb mixture. Namely, we take components 1 and 2 as the hyperfine states $|F = 1, m_F = 1\rangle$ of ^{23}Na and ^{87}Rb atoms, respectively, which features an interspecies Feshbach resonance at $B = 347.65\text{G}$. These two components can support a binary droplet as been successfully observed in experiment [14]. For component 3, we take it as another hyperfine state $|F = 1, m_F = 0\rangle$ of ^{87}Rb atom, which can be coupled to component 2 via a Rabi field. Throughout this paper, we consider the ^{23}Na - ^{87}Rb mixture near $B \sim 349.28\text{G}$, with fixed scattering lengths $(a_{11}, a_{22}, a_{33}, a_{12}, a_{13}, a_{23}) = (60.1, 100.1, 100.9, -123.2, 89.7, 100.4)a_0$ (a_0 is the Bohr radius) [14, 53]. In this regime, we have $g_{12} < -\sqrt{g_{11}g_{22}}$ and thus (1,2) droplet can be supported in vacuum. Moreover, we consider flexible strengths of Ω and δ , which can be tuned conveniently by the intensity and frequency of the Rabi field.

III. MEAN-FIELD ANALYSIS

In this section, we analyze the mean-field stability of three-component bosons against density fluctuations.

First, under the mean-field treatment, we replace the field operators by $\psi_2 = \sqrt{n_{23}} \sin \frac{\phi}{2}$, $\psi_3 = \sqrt{n_{23}} \cos \frac{\phi}{2}$ and $\psi_1 = \sqrt{n_1}$. Here we have assumed homogeneous densities n_i ($i = 1, 2, 3$), and $n_{23} \equiv n_2 + n_3$. The density imbalance between components 2 and 3 is characterized by the polarization $S \equiv (n_3 - n_2)/n_{23} = \cos \phi$. Then we have the mean-field energy density

$$\begin{aligned} \mathcal{E}_{\text{MF}} &= -(\Omega\sqrt{1-S^2} + \delta S)n_{23} + \left[\frac{g_{22} + g_{33} - 2g_{23}}{8} S^2 \right. \\ &\quad \left. - \frac{g_{22} - g_{33}}{4} S + \frac{g_{22} + g_{33} + 2g_{23}}{8} \right] n_{23}^2 \\ &\quad + \frac{1}{2} g_{11} n_1^2 + \left[\frac{g_{13} - g_{12}}{2} S + \frac{g_{13} + g_{12}}{2} \right] n_1 n_{23}. \end{aligned} \quad (2)$$

The equilibrium polarization S , as a function of n_{12} and n_3 , is determined by

$$\frac{\partial \mathcal{E}_{\text{MF}}}{\partial S} = 0, \quad (3)$$

which further gives \mathcal{E}_{MF} as a function of n_1 and n_{23} .

The mean-field stability can be examined by evaluating the second-order variation of \mathcal{E}_{MF} with respect to small density fluctuations

$$\delta^2 \mathcal{E}_{\text{MF}} = \frac{1}{2} \sum_{\alpha\beta} g_{\alpha\beta}^{\text{eff}} \delta n_\alpha \delta n_\beta, \quad (4)$$

where $\alpha, \beta = \{1, 23\}$ and the effective interaction strength is defined as

$$g_{\alpha\beta}^{\text{eff}} = \frac{\partial^2 \mathcal{E}_{\text{MF}}}{\partial n_\alpha \partial n_\beta}. \quad (5)$$

Diagonalization of $\delta^2 \mathcal{E}_{\text{mf}}$ in (4) yields the eigen fluctuation modes, from which one can determine the mean-field stability of the system. Notably, the presence of Rabi coupling ($\Omega \neq 0$) gives rise to a highly non-linear dependence of \mathcal{E}_{MF} on $\{n_1, n_{23}\}$, thereby leading to density-dependent stability even at the mean-field level.

Explicitly, (4) can be diagonalized as

$$\delta^2 \mathcal{E}_{\text{MF}} = \tilde{g}_1 \delta \tilde{n}_1^2 + \tilde{g}_{23} \delta \tilde{n}_{23}^2, \quad (6)$$

where \tilde{n}_1 and \tilde{n}_{23} are the two eigen-modes of fluctuations, and \tilde{g}_1 and \tilde{g}_{23} are their according eigenvalues. A stable mean-field phase corresponds to all these modes having positive eigenvalues, i.e., $\tilde{g}_1 > 0, \tilde{g}_{23} > 0$ in (6) and $g_{\alpha\alpha}^{\text{eff}} > 0$ in (4). If any of these conditions breaks down, the system tends to become unstable against density fluctuations.

In Fig. 2, we map out the mean-field phase diagram in (n_1, n_{23}) plane at typical values of Ω and $\delta = 0$. Apart from the mean-field stable regime (marked ‘stable’), we find two unstable regions towards mean-field collapse. Specifically, ‘collapse-I’ corresponds to $g_{11}^{\text{eff}} < 0$, which

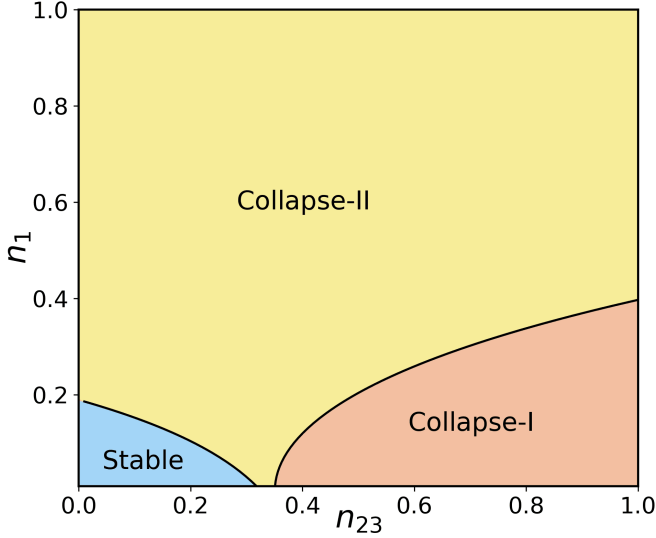


FIG. 2. Mean-field phase diagram of three-component bosons in (n_1, n_{23}) plane. Three phases are identified: a stable miscible phase ('stable'), and two unstable phases towards collapse of component-1 ('collapse-I') and collapse of all components ('collapse-II'). Here we take the Na-Rb mixture at $\delta = 0$, and the densities are scaled by Ω/g_{11} .

gives the collapse of component-1, and 'collapse-II' corresponds to $\tilde{g}_1\tilde{g}_{23} < 0$ while $g_{\alpha\alpha}^{\text{eff}} > 0$, which gives the collapse of all three components.

Starting from the stable region at small n_1 and n_{23} , we can see that increasing n_{23} will drive the system to 'collapse-I', while increasing n_1 or both densities drives it to 'collapse-II'. This can be understood as follows.

In the low-density limit of (n_1, n_{23}) , the single-particle physics dominates and the whole system is stable because all $g_{ii} > 0$. For a fixed small n_1 , increasing n_{23} introduces a correction to the effective 1-1 coupling strength: $\Delta g_{11} = \frac{g_{13}-g_{12}}{2} \frac{\partial S}{\partial n_1} n_{23}$, as seen from the mean-field energy in Eq. (4). Because the 1-2 attraction favors component-2 over component-3, we have $\frac{\partial S}{\partial n_1} < 0$, making this correction negative and finally leading to $g_{11}^{\text{eff}} = g_{11} + \Delta g_{11} < 0$, i.e., the 'collapse-I' region. As both n_1 and n_{23} continue to increase, the interaction energy becomes dominant, and due to the strong 1-2 attraction the system is driven into the 'collapse-II' region, where all three components undergo mean-field collapse. This implies the formation of a three-component droplet when the LHY energy from quantum fluctuations is included, as to be discussed in the next section.

IV. THREE-COMPONENT QUANTUM DROPLET

We now proceed with the formation of three-component droplets by incorporating the effect of quantum fluctuations. Based on the standard Bogoliubov theory, we expand the field operator as:

$$\psi_i(\mathbf{r}) = \sqrt{n_i} + \frac{1}{\sqrt{V}} \sum_{\mathbf{k} \neq 0} e^{i\mathbf{k}\mathbf{r}} a_{i\mathbf{k}}, \quad (7)$$

where $a_{i\mathbf{k}}$ is the fluctuation operator for component- i bosons at momentum \mathbf{k} . The Hamiltonian in (1) can then be reduced to bilinear form:

$$\frac{H}{V} = \mathcal{E}_{\text{MF}} + \frac{1}{V} \sum_{\mathbf{p} \neq 0}' \left[\phi^\dagger h_{\mathbf{p}} \phi - \sum_{i=1}^3 (\epsilon_{i\mathbf{p}} + n_i g_{ii}) + \Omega \frac{n_2 + n_3}{\sqrt{n_2 n_3}} \right] \quad (8)$$

where $\sum_{\mathbf{p}}'$ denotes the summation only in half of momentum space; $\mathcal{E}_{\text{MF}} = \frac{1}{2} \sum_{i,j} g_{ij} n_i n_j - 2\Omega \sqrt{n_2 n_3} + \delta(n_2 - n_3)$, $\epsilon_{i\mathbf{p}} = \mathbf{p}^2/2m_i$, $\phi = (a_{1\mathbf{p}} \ a_{2\mathbf{p}} \ a_{3\mathbf{p}} \ a_{1-\mathbf{p}}^\dagger \ a_{2-\mathbf{p}}^\dagger \ a_{3-\mathbf{p}}^\dagger)^T$ and

$$h_{\mathbf{p}} = \begin{pmatrix} \epsilon_{1\mathbf{p}} + n_1 g_{11} & g_{12} \sqrt{n_1 n_2} & g_{13} \sqrt{n_1 n_3} & n_1 g_{11} & g_{12} \sqrt{n_1 n_2} & g_{13} \sqrt{n_1 n_3} \\ g_{12} \sqrt{n_1 n_2} & \epsilon_{2\mathbf{p}} + \Omega \sqrt{\frac{n_3}{n_2}} + n_2 g_{22} & g_{23} \sqrt{n_2 n_3} - \Omega & g_{12} \sqrt{n_1 n_2} & n_2 g_{22} & g_{23} \sqrt{n_2 n_3} \\ g_{13} \sqrt{n_1 n_3} & g_{23} \sqrt{n_2 n_3} - \Omega & \epsilon_{3\mathbf{p}} + \Omega \sqrt{\frac{n_2}{n_3}} + n_3 g_{33} & g_{13} \sqrt{n_1 n_3} & g_{23} \sqrt{n_2 n_3} & n_3 g_{33} \\ n_1 g_{11} & g_{12} \sqrt{n_1 n_2} & g_{13} \sqrt{n_1 n_3} & \epsilon_{1\mathbf{p}} + n_1 g_{11} & g_{12} \sqrt{n_1 n_2} & g_{13} \sqrt{n_1 n_3} \\ g_{12} \sqrt{n_1 n_2} & n_2 g_{22} & g_{23} \sqrt{n_2 n_3} & g_{12} \sqrt{n_1 n_2} & \epsilon_{2\mathbf{p}} + \Omega \sqrt{\frac{n_3}{n_2}} + n_2 g_{22} & g_{23} \sqrt{n_2 n_3} - \Omega \\ g_{13} \sqrt{n_1 n_3} & g_{23} \sqrt{n_2 n_3} & n_3 g_{33} & g_{13} \sqrt{n_1 n_3} & g_{23} \sqrt{n_2 n_3} - \Omega & \epsilon_{3\mathbf{p}} + \Omega \sqrt{\frac{n_2}{n_3}} + n_3 g_{33} \end{pmatrix}. \quad (9)$$

The Bogoliubov modes $\{E_{i\mathbf{p}}\}$ can be obtained by diagonalizing matrix $\Gamma h_{\mathbf{p}}$, with $\Gamma = \text{diag}(1, 1, 1, -1, -1, -1)$. Finally we arrive at the LHY energy density

$$\mathcal{E}_{\text{LHY}} = \frac{1}{2V} \sum_{\mathbf{p} \neq 0}' \left[\sum_{i=1}^3 (E_{i\mathbf{p}} - \epsilon_{i\mathbf{p}} - n_i g_{ii} + \sum_{j=1}^3 \frac{2m_{ij} g_{ij}^2 n_i n_j}{\mathbf{p}^2}) - \Omega \frac{n_2 + n_3}{\sqrt{n_2 n_3}} \right]. \quad (10)$$

The total energy density is then:

$$\mathcal{E}(S, n_1, n_{23}) = \mathcal{E}_{\text{MF}} + \mathcal{E}_{\text{LHY}}. \quad (11)$$

Minimizing \mathcal{E} with respect to the spin polarization S , we can express \mathcal{E} solely as a function of the densities n_1 and n_{23} . This then determines the chemical potentials $\mu_1 = \partial\mathcal{E}/\partial n_1$ and $\mu_{23} = \partial\mathcal{E}/\partial n_{23}$, and a self-bound droplet in vacuum requires

$$\mathcal{P}(n_1, n_{23}) \equiv \mu_1 n_1 + \mu_{23} n_{23} - \mathcal{E}(n_1, n_{23}) = 0. \quad (12)$$

Apparently, the single condition in (12) cannot uniquely determine n_1 and n_{23} . In general, one additionally requires an energy minimum under zero-pressure conditions. Combining this requirement with (12) yields a unique solution n_1, n_{23} for the droplet. Furthermore, to ensure that such a self-bound droplet is stable, one

must have

$$\mu_1 \leq \mu_1^{(0)}, \quad \mu_{23} \leq \mu_{23}^{(0)}, \quad (13)$$

with $\mu_1^{(0)} = 0$ and $\mu_{23}^{(0)} = -\sqrt{\Omega^2 + \delta^2}$ the chemical potentials in vacuum (i.e., for a single-particle system). The inequality $\mu_\alpha \leq \mu_\alpha^{(0)}$ ensures that an additional α -atom prefers to stay with the droplet rather than in the vacuum, effectively preventing atom loss from the droplet to the surrounding environment. In the limiting case where $\mu_\alpha = \mu_\alpha^{(0)}$, the droplet and vacuum reach equilibrium for the α -component. This is also a stable solution, corresponding to liquid-gas coexistence as studied previously [26, 27].

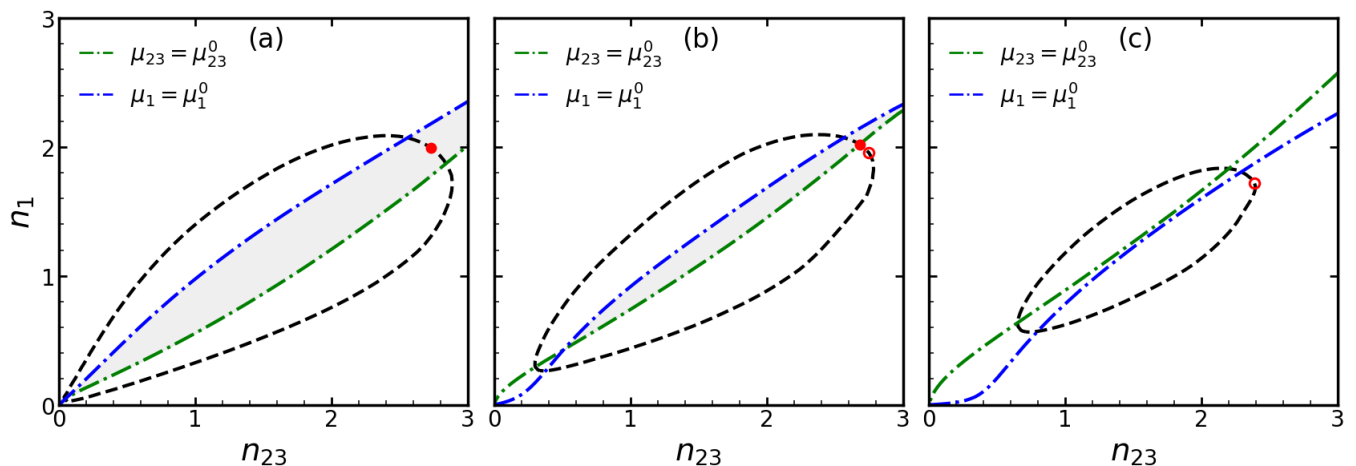


FIG. 3. Quantum droplet solutions in the (n_1, n_{23}) plane at fixed $\delta = 0$ and varying $\Omega/(\hbar\nu_0) = 0.2$ (a), 0.8 (b), and 1.4 (c), with $\nu_0 = 20$ kHz. The black dashed curve shows the zero-pressure contour, while the blue and green dash-dotted curves denote the locations where the chemical potentials meet the vacuum values: $\mu_\alpha = \mu_\alpha^{(0)}$. The shaded region marks the regime where Eq. (13) is satisfied. The red solid dot indicates the stable droplet solution on the zero-pressure contour. The red hollow dot marks the global minimum on the zero-pressure contour when it lies outside the stable region. In these plots, stable droplets exist in (a,b) but not in (c). The density unit is $\hbar\nu_0/g_{11}$, and the other parameters are the same as specified in the main text for the Na-Rb system.

In Fig. 3, we show typical droplet solutions in the (n_1, n_{23}) plane at $\delta = 0$ and varying Ω . For small Ω in Fig. 3(a), the red solid dot represents the energy minimum on the zero-pressure contour, which lies within the shaded region satisfying the chemical potential condition (13). It therefore represents a stable droplet solution. As Ω increases, the shaded area becomes narrower, and the global minimum of the zero-pressure contour can move outside the shaded region (see the red hollow dot in

Fig. 3(b)). Nevertheless, the zero-pressure contour can still cross the shaded area, and one can identify the stable solution as the lowest-energy point on the contour within the area, as shown by the solid red dot in Fig. 3(b). Upon further increasing Ω , the shaded area disappears and a stable droplet solution can no longer be supported (see Fig. 3(c)).

As indicated in Fig. 3, there is an upper bound on Ω for achieving stable three-component droplets. Physi-

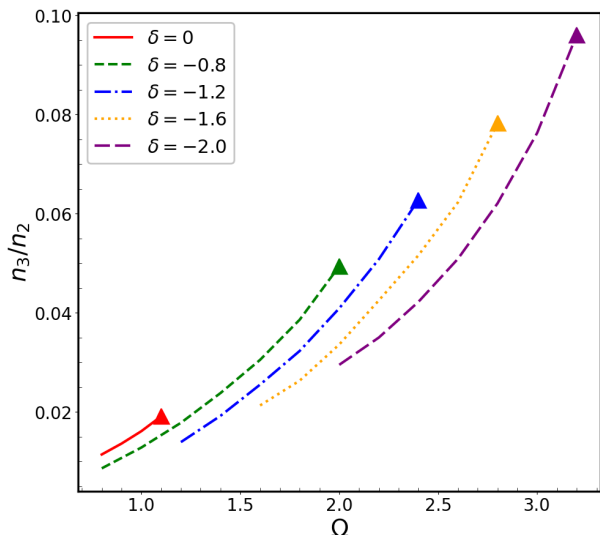


FIG. 4. Density ratio n_3/n_2 as a function of Ω at different detunings $\delta = 0, 0.8, 1.2, 1.6, 2.0$. The triangles mark the upper bounds of Ω and n_3/n_2 for a stable three-component droplet. The units of Ω and δ are $\hbar\nu_0$, with $\nu_0 = 20$ kHz. Other parameters are the same as specified in the main text for the Na-Rb system.

cally, this can be understood as follows. As Ω increases, components 2 and 3 become more strongly coupled, and therefore more 3 atoms join the droplet, as shown by the increase in n_3/n_2 in Fig. 4. Since interactions between component 3 and the other components are all repulsive, the increase in n_3 introduces more repulsive forces into the system and eventually destabilizes the self-bound droplet. Consequently, along with the upper bound on Ω , there is an upper bound on n_3/n_2 for a stable droplet. As shown in Fig. 4, at $\delta = 0$, the upper bound of n_3/n_2 is about 2%, meaning that the three-component droplet is still dominated by the (1,2) binary droplet, with only a tiny fraction of component 3.

Interestingly, the fraction of component 3 can be efficiently enhanced by switching on a finite detuning δ between it and component 2. As shown in Fig. 4, when δ is tuned negative and its magnitude increased, a stable three-component droplet is allowed over a broader range of Ω , enabling a higher fraction of 3 (or n_3/n_2) at the upper bound of Ω . For instance, at $\delta/\hbar = -40$ kHz, a stable droplet solution can extend to $\Omega = 64$ kHz, at which n_3/n_2 can reach about 10%. Such δ -stabilized droplet formation can be understood as follows. When a finite δ is turned on, the shift in μ_{23} is dominated by $-\delta S$, as seen from the mean-field energy in Eq. (2). Given $S < 0$ ($n_3 < n_2$), this shift is negative for $\delta < 0$, meaning that μ_{23} decreases linearly as $|\delta|$ increases. On the other hand, the vacuum value $\mu_{23}^{(0)}$ decreases quadratically as $|\delta|$ increases. Consequently, at small negative δ , the condition $\mu_{23} < \mu_{23}^{(0)}$ is more easily satisfied compared to the case $\delta = 0$. In other words, the shaded area in Fig. 3

(satisfying (13)) broadens as δ becomes more negative, thereby favoring the droplet formation.

In above we have discussed the properties of three-component quantum droplet in the thermodynamic limit ($N_i, V \rightarrow \infty$ with fixed $n_i \equiv N_i/V$). However, in realistic ultracold systems, atom numbers are finite and one must consider finite-size effects. To describe a finite-size droplet, we employ the extended Gross-Pitaevskii (GP) equations under the local density approximation:

$$\begin{aligned} i\hbar \frac{\partial}{\partial t} \psi_1 &= \left(-\frac{\hbar^2 \nabla^2}{2m_1} + \sum_i g_{1i} n_i + \frac{\partial \mathcal{E}_{\text{LHY}}}{\partial n_1} \right) \psi_1, \\ i\hbar \frac{\partial}{\partial t} \psi_2 &= \left(-\frac{\hbar^2 \nabla^2}{2m_2} + \sum_i g_{2i} n_i + \delta + \frac{\partial \mathcal{E}_{\text{LHY}}}{\partial n_2} \right) \psi_2 - \Omega \psi_3, \\ i\hbar \frac{\partial}{\partial t} \psi_3 &= \left(-\frac{\hbar^2 \nabla^2}{2m_3} + \sum_i g_{3i} n_i - \delta + \frac{\partial \mathcal{E}_{\text{LHY}}}{\partial n_3} \right) \psi_3 - \Omega \psi_2. \end{aligned} \quad (14)$$

with $n_i(\mathbf{r}) = |\psi_i(\mathbf{r})|^2$. Based on the coupled GP equations, we have obtained the ground state by performing imaginary-time evolutions. In view of the underlying symmetry, we consider only a spherically symmetric droplet. This configuration allows the largest density overlap between different components and is therefore believed to be energetically favorable over other asymmetric configurations for a miscible three-component state.

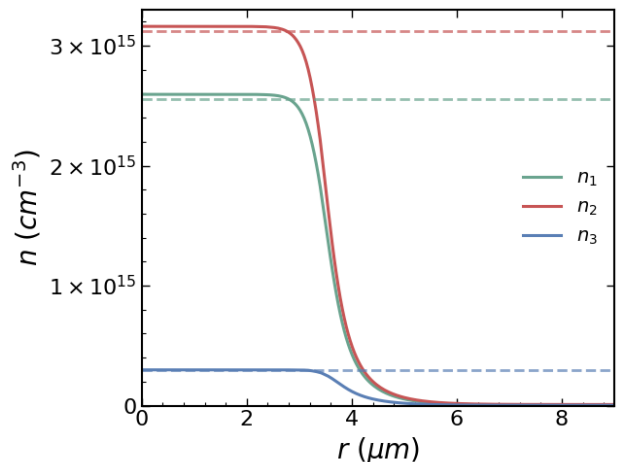


FIG. 5. Density profiles of a three-component quantum droplet at $\delta = -2$ and $\Omega = 3.2$. The units of Ω and δ are $\hbar\nu_0$, with $\nu_0 = 20$ kHz. The solid lines are from numerical simulations based on (14), with particle numbers $(N_1, N_{23})/10^5 = (9.1, 6.5)$. The horizontal dashed lines show equilibrium densities in the thermodynamic limit.

In Fig. 5, we show typical density profiles of a three-component droplet from GP simulations, corresponding to the highest triangle point in Fig. 4. All three components exhibit flat-top densities in the bulk, which match very well with the equilibrium densities in the thermodynamic limit (see dashed horizontal lines in Fig. 5). We have also tested cases with larger Ω where the thermo-

dynamic analysis does not predict a stable droplet, as in the example shown in Fig. 3(c). In those cases, the GP simulations do not yield a stable self-bound solution, as expected. These results verify our theoretical analyses of the stabilization conditions for a three-component quantum droplet.

V. SUMMARY AND OUTLOOK

In summary, we have shown that Rabi coupling can facilitate the formation of three-component quantum droplets even when only one inter-species attraction exists among the three components. Specifically, the Rabi field couples one component of a binary droplet to a third component, thereby gluing all three components together as a self-bound object. Increasing the Rabi coupling leads to a higher fraction of the third component, but also destabilizes the droplet due to the involvement of more repulsive forces. Furthermore, we show that a finite magnetic detuning between the Rabi-coupled components can enhance the stability of the three-component droplet and conveniently tune the upper fraction of the third component. All these results can be readily detected in current cold-atom experiments on Na-Rb mixtures, as well as in other boson-boson mixtures with similar setups of external fields and interatomic interactions.

In this work, all calculations have been performed in a single magnetic field corresponding to a fixed a_{12} . Since the three-component droplet is ultimately stabilized by the attractive interaction between components 1 and 2, a natural expectation is that making a_{12} more negative — by tuning the magnetic field closer to the Feshbach resonance — would strengthen the attractive mean-field contribution and thereby allow the system to accommo-

date a larger fraction of the repulsive component 3 before the droplet is destabilized. This would effectively widen the stability window in Ω and enlarge the accessible range of three-component droplet compositions. We have numerically verified this expectation for a value of a_{12} that is more negative than the present case. A systematic study of how the droplet phase diagram evolves with a_{12} remains an interesting direction for future work.

Beyond the three-component framework, our results outline a general route for stabilizing multi-component droplets. Namely, one can first prepare a basic binary droplet and then couple it to additional components using suitable single-particle fields. Here, the single-particle field serves as a bridge between the existing droplet and the additional components, thereby allowing the formation of larger self-bound objects with more components. On the other hand, a side effect of such single-particle fields is that they may effectively weaken the binding strength of the basic droplet and eventually destroy the self-bound state, as shown in the present work at large Rabi coupling strengths. In the future, it will be interesting to explore the collective excitations and dynamical formation of such multi-component droplets, which are expected to reveal the intrinsic inter-species correlations in a more visible way.

Data that support the findings of this article are openly available [54].

ACKNOWLEDGMENTS

This work is supported by National Natural Science Foundation of China (12525412, 92476104, 12134015) and Innovation Program for Quantum Science and Technology (2024ZD0300600). D.W. is supported by Hong Kong RGC (GRF 14304024 and CRF C4050-23G).

-
- [1] D. S. Petrov, *Quantum Mechanical Stabilization of a Collapsing Bose-Bose Mixture*, Phys. Rev. Lett. **115**, 155302 (2015).
 - [2] I. Ferrier-Barbut, H. Kadau, M. Schmitt, M. Wenzel, T. Pfau, *Observation of Quantum Droplets in a Strongly Dipolar Bose Gas*, Phys. Rev. Lett. **116**, 215301 (2016).
 - [3] M. Schmitt, M. Wenzel, F. Böttcher, I. Ferrier-Barbut, T. Pfau, *Self-bound droplets of a dilute magnetic quantum liquid*, Nature **539**, 259 (2016).
 - [4] L. Chomaz, S. Baier, D. Petter, M. J. Mark, F. Wächtler, L. Santos, F. Ferlaino, *Quantum-fluctuation-driven crossover from a dilute Bose-Einstein condensate to a macrodroplet in a dipolar quantum fluid*, Phys. Rev. X **6**, 041039 (2016).
 - [5] L. Tanzi, E. Lucioni, F. Famà, J. Catani, A. Fioretti, C. Gabbanini, R. N. Bisset, L. Santos, G. Modugno, *Observation of a Dipolar Quantum Gas with Metastable Supersolid Properties*, Phys. Rev. Lett. **122**, 130405 (2019).
 - [6] F. Böttcher, J. N. Schmidt, M. Wenzel, J. Hertkorn, M. Guo, T. Langen, T. Pfau, *Transient Supersolid Properties in an Array of Dipolar Quantum Droplets*, Phys. Rev. X **9**, 011051 (2019).
 - [7] L. Chomaz, D. Petter, P. Ilzhöfer, G. Natale, A. Trautmann, C. Politi, G. Durastante, R. M. W. van Bijnen, A. Patscheider, M. Sohmen, M. J. Mark, F. Ferlaino, *Long-Lived and Transient Supersolid Behaviors in Dipolar Quantum Gases*, Phys. Rev. X **9**, 021012 (2019).
 - [8] C. R. Cabrera, L. Tanzi, J. Sanz, B. Naylor, P. Thomas, P. Cheiney, L. Tarruell, *Quantum liquid droplets in a mixture of Bose-Einstein condensates*, Science **359**, 301 (2018).
 - [9] P. Cheiney, C. R. Cabrera, J. Sanz, B. Naylor, L. Tanzi, L. Tarruell, *Bright Soliton to Quantum Droplet Transition in a Mixture of Bose-Einstein Condensates*, Phys. Rev. Lett. **120**, 135301 (2018).
 - [10] G. Semeghini, G. Ferioli, L. Masi, C. Mazzinghi, L. Wolswijk, F. Minardi, M. Modugno, G. Modugno, M. Inguscio, M. Fattori, *Self-Bound Quantum Droplets of Atomic Mixtures in Free Space*, Phys. Rev. Lett. **120**, 235301 (2018).

- [11] C. D'Errico, A. Burchianti, M. Prevedelli, L. Salasnich, F. Ancilotto, M. Modugno, F. Minardi, C. Fort, *Observation of quantum droplets in a heteronuclear bosonic mixture*, Phys. Rev. Res. **1**, 033155 (2019).
- [12] A. Burchianti, C. D'Errico, M. Prevedelli, L. Salasnich, F. Ancilotto, M. Modugno, F. Minardi, C. Fort, *A Dual-Species Bose-Einstein Condensate with Attractive Interspecies Interactions*, Condens. Matter **5**, 21 (2020).
- [13] G. Ferioli, G. Semeghini, S. Terradas-Briansó, L. Masi, M. Fattori, and M. Modugno, *Dynamical formation of quantum droplets in a ^{39}K mixture*, Phys. Rev. Research **2**, 013269 (2020).
- [14] Z. Guo, F. Jia, L. Li, Y. Ma, J. M. Hutson, X. Cui, D. Wang, *Lee-Huang-Yang effects in the ultracold mixture of ^{23}Na and ^{87}Rb with attractive interspecies interactions*, Phys. Rev. Res. **3**, 033247 (2021).
- [15] L. Cavicchioli, C. Fort, F. Ancilotto, M. Modugno, F. Minardi, and A. Burchianti, *Dynamical Formation of Multiple Quantum Droplets in a Bose-Bose Mixture*, Phys. Rev. Lett. **134**, 093401 (2025).
- [16] M. Tylutki, G. E. Astrakharchik, B. A. Malomed, and D. S. Petrov, *Collective Excitations of a One-Dimensional Quantum Droplet*, Phys. Rev. A **101**, 051601(R) (2020).
- [17] H. Hu and X.-J. Liu, *Collective excitations of a spherical ultradilute quantum droplet*, Phys. Rev. A **102**, 053303 (2020).
- [18] P. Stürmer, M. Nilsson Tengstrand, R. Sachdeva, and S. M. Reimann, *Breathing mode in two-dimensional binary self-bound Bose-gas droplets*, Phys. Rev. A **103**, 053302 (2021).
- [19] E. Orignac, S. De Palo, L. Salasnich, and R. Citro, *Breathing mode of a quantum droplet in a quasi-one-dimensional dipolar Bose gas*, Phys. Rev. A **109**, 043316 (2024).
- [20] Y. Fei, X. Du, X.-L. Chen, and Y. Zhang, *Collective excitations in two-dimensional harmonically trapped quantum droplets*, Phys. Rev. A **109**, 053309 (2024).
- [21] D. S. Petrov and G. E. Astrakharchik, *Ultradilute Low-Dimensional Liquids*, Phys. Rev. Lett. **117**, 100401 (2016).
- [22] L. Parisi and S. Giorgini, *Quantum droplets in one-dimensional Bose mixtures: A quantum Monte Carlo study*, Phys. Rev. A **102**, 023318 (2020).
- [23] X. Du, Y. Fei, X.-L. Chen, and Y. Zhang, *Ground-state properties and Bogoliubov modes of a harmonically trapped one-dimensional quantum droplet*, Phys. Rev. A **108**, 033312 (2023).
- [24] X. Cui and Y. Ma, *Droplet under confinement: Competition and coexistence with a soliton bound state*, Phys. Rev. Research **3**, L012027 (2021).
- [25] J. C. Pelayo, G. Bougas, T. Fogarty, T. Busch, and S. I. Mistakidis, *Phases and dynamics of quantum droplets in the crossover to two-dimensions*, SciPost Phys. **18**, 129 (2025).
- [26] Q. Gu and X. Cui, *Liquid-gas transition and coexistence in ground-state bosons with spin twist*, Phys. Rev. A **107**, L031303 (2023).
- [27] L. He, H. Li, W. Yi, and Z.-Q. Yu, *Quantum Criticality of Liquid-Gas Transition in a Binary Bose Mixture*, Phys. Rev. Lett. **130**, 193001 (2023).
- [28] G. Spada, S. Pilati, and S. Giorgini, *Attractive Solution of Binary Bose Mixtures: Liquid-Vapor Coexistence and Critical Point*, Phys. Rev. Lett. **131**, 173404 (2023).
- [29] Y. Li, Z. Chen, Z. Luo, C. Huang, H. Tan, W. Pang, B. A. Malomed, *Two-dimensional vortex quantum droplets*, Phys. Rev. A **98**, 063602 (2018).
- [30] X. Zhang, X. Xu, Y. Zheng, Z. Chen, B. Liu, C. Huang, B. A. Malomed, Y. Li, *Semidiscrete quantum droplets and vortices*, Phys. Rev. Lett. **123**, 133901 (2019).
- [31] M. N. Tengstrand, P. Stürmer, E. Karabulut, S. M. Reimann, *Rotating binary Bose-Einstein condensates and vortex clusters in quantum droplets*, Phys. Rev. Lett. **123**, 160405 (2019).
- [32] M. Caldara, F. Ancilotto, *Vortices in quantum droplets of heteronuclear Bose mixtures*, Phys. Rev. A **105**, 063328 (2022).
- [33] Q. Gu, X. Cui, *Self-bound Vortex Lattice in a Rapidly Rotating Quantum Droplet*, Phys. Rev. A **108**, 063302 (2023).
- [34] T. A. Yoğurt, U. Tanyeri, A. Keleş, M. Ö. Oktel, *Vortex lattices in strongly confined quantum droplets*, Phys. Rev. A **108**, 033315 (2023).
- [35] G. E. Astrakharchik, B. A. Malomed, *Dynamics of one-dimensional quantum droplets*, Phys. Rev. A **98**, 013631 (2018).
- [36] G. Ferioli, G. Semeghini, L. Masi, G. Giusti, G. Modugno, M. Inguscio, A. Gallemini, A. Recati, M. Fattori, *Collisions of Self-Bound Quantum Droplets*, Phys. Rev. Lett. **122**, 090401 (2019).
- [37] V. Cikojević, L. Vranješ Markić, M. Pi, M. Barranco, F. Ancilotto, J. Boronat, *Dynamics of equilibration and collisions in ultradilute quantum droplets*, Phys. Rev. Res. **3**, 043139 (2021).
- [38] C. Fort, M. Modugno, *Self-evaporation dynamics of quantum droplets in a ^{41}K - ^{87}Rb mixture*, Appl. Sci. **11**, 866 (2021).
- [39] Y. Ma and X. Cui, *Quantum-fluctuation-driven dynamics of droplet splashing, recoiling, and deposition in ultracold binary Bose gases*, Phys. Rev. Research **5**, 013100 (2023).
- [40] I. A. Englezos, S. I. Mistakidis, and P. Schmelcher, *Correlated dynamics of collective droplet excitations in a one-dimensional harmonic trap*, Phys. Rev. A **107**, 023320 (2023).
- [41] Y. Li, Z. Luo, Y. Liu, Z. Chen, C. Huang, S. Fu, H. Tan, and B. A. Malomed, *Two-dimensional solitons and quantum droplets supported by competing self- and cross-interactions in spin-orbit-coupled condensates*, New J. Phys. **19**, 113043 (2017).
- [42] X. Cui, *Spin-orbit-coupling-induced quantum droplet in ultracold Bose-Fermi mixtures*, Phys. Rev. A **98**, 023630 (2018).
- [43] J. Sánchez-Baena, J. Boronat, and F. Mazzanti, *Supersolid striped droplets in a Raman spin-orbit-coupled system*, Phys. Rev. A **102**, 053308 (2020).
- [44] Y. Xiong and L. Yin, *Self-Bound Quantum Droplet with Internal Stripe Structure in One-Dimensional Spin-Orbit-Coupled Bose Gas*, Chin. Phys. Lett. **38**, 070301 (2021).
- [45] L. Lavoine, A. Hammond, A. Recati, D. S. Petrov, and T. Bourdel, *Beyond-Mean-Field Effects in Rabi-Coupled Two-Component Bose-Einstein Condensate*, Phys. Rev. Lett. **127**, 203402 (2021).
- [46] T. A. Yoğurt, A. Keleş, and M. Ö. Oktel, *Polarized Rabi-coupled and spinor boson droplets*, Phys. Rev. A **107**, 023322 (2023).

- [47] T. Luo and X. Cui, *Chiral quantum droplet in a spin-orbit-coupled Bose gas*, Phys. Rev. A **112**, 043312 (2025).
- [48] Y. Ma, C. Peng, and X. Cui, *Borromean Droplet in Three-Component Ultracold Bose Gases*, Phys. Rev. Lett. **127**, 043002 (2021).
- [49] Y. Ma and X. Cui, *Shell-Shaped Quantum Droplet in a Three-Component Ultracold Bose Gas*, Phys. Rev. Lett. **134**, 043402 (2025).
- [50] G. Bighin, A. Burchianti, F. Minardi, and T. Macrì, *Impurity in a heteronuclear two-component Bose mixture*, Phys. Rev. A **106**, 023301 (2022).
- [51] I. A. Englezos, P. Schmelcher, and S. I. Mistakidis, *Multi-component one-dimensional quantum droplets across the mean-field stability regime*, SciPost Phys. **19**, 133 (2025).
- [52] I. A. Englezos, E. G. Charalampidis, P. Schmelcher, and S. I. Mistakidis, *Stability and mixed phases of three-component droplets in one dimension*, arXiv:2601.04950 (2026).
- [53] Z. Guo, F. Jia, B. Zhu, L. Li, J. M. Hutson, D. Wang, *Improved characterization of Feshbach resonances and interaction potentials between ^{23}Na and ^{87}Rb atoms*, Phys. Rev. A **105**, 023313 (2022).
- [54] X. Ding, D. Wang and X. Cui, *Data for Rabi-coupling-induced three-component quantum droplet in ultracold Bose gases*, <https://doi.org/10.5281/zenodo.19795275>.